Controlling Modes using VCSEL-Based Photonic Crystal Heterostructures

L. D. A. Lundeberg and E. Kapon
Ecole Polytechnique Fédérale de Lausanne (EPFL), Laboratory of Physics of Nanostructures,
CH-1015 Lausanne, Switzerland
lars.lundeberg@epfl.ch

Abstract: *Photonic crystal heterostructures can be used to tailor the optical supermodes in arrays of vertical-cavity surface emitting lasers. Merging mode confinement effects with active control of the photonic properties opens up the way for new optical switching devices utilizing wide-area coherent light sources.*

Introduction

One of the advantages of vertical-cavity surface-emitting lasers (VCSELs) is the ability to couple several lasers together in two-dimensional (2D) arrays. Such arrays may lase in a phase-locked mode providing wide-area coherent light with laser emission contained in diffraction limited far-field pattern [1]. Along with the appealing possibilities for novel photonic devices, two-dimensional arrays of VCSELs can be regarded as a model photonic lattice [2-4], and the concept of photonic crystals (PhC) has successfully been applied for the study of photonic disorder [5] and photonic band structure [6] in this type of arrays. Furthermore, concatenating VCSEL-arrays with different dispersion properties can yield PhC heterostructures (PhCHs), with which the photonic envelope functions can be controlled using PhC heterojunctions [7-9]. In particular, such PhCHs can confine the photonic states in a 2D "island" domain of low photonic band-gap material surrounded by a "sea" of higher photonic band-gap (Fig 1). In this way, it is possible to tailor the distribution of the transverse lasing mode, which should find applications in novel optical switches and routers.

In this work, we combine photonic envelope function confinement with active control of the gain distribution in VCSEL-based PhCHs. Tweaking PhCH domains in and out of coupling significantly alters the far-field pattern, which make possible active beam switching and wavelength tuning with wide-area VCSEL-arrays

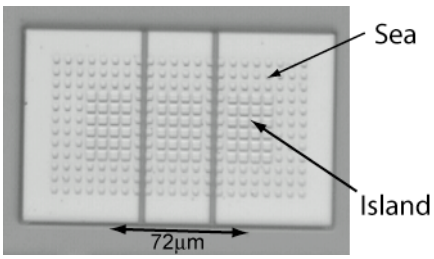

Fig. 1: Optical micrograph (top view) of a PhCH containing three 4x6 photonic islands defined on a VCSEL wafer.

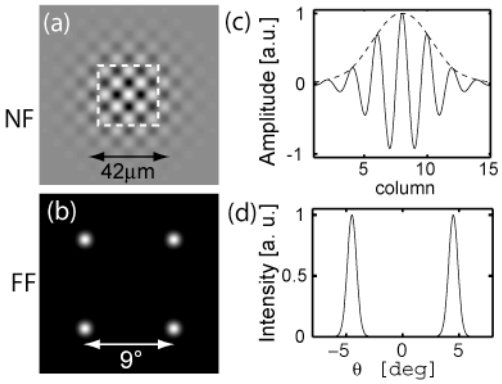

Fig. 2: (a) Calculated near and far-field (b) patterns of 5×5 photonic island (dashed square). (c) Near field line scan across the center of (a). (d) Far-field line scan across the main lobes. λ=940 nm, Λ=6 μm, Au pixel size 4.9×4.9μm^2, (island), 3×3μm^2 (sea).

Coupled Heterostructures

Figure 2 illustrates confinement of the envelope function in a single photonic island [8]. The PhCH consists of an island comprising 5×5 high reflectivity Au pixels (4.9×4.9μm^2 on a 6μm pitch) surrounded by a low reflectivity Cr grid, deposited on a conventional InGaAs/GaAs/AlGaAs VCSEL wafer [1] emitting at 943nm wavelength. The island is surrounded by a sea of the same square lattice structure but of smaller Au pixel size (3×3μm^2). The lowest loss supermode maintains the out-of-phase modulation across the heterojunction and the resulting far-field pattern exhibits four main far-field lobes.

As a natural extension to the single photonic island system, we consider two embedded PhC islands in a PhC sea and study the coupling between them. Following the analogy with semiconductor heterostructures, the system of two separated PhC domains can be regarded as two coupled photonic wells. As such, two equal-sized photonic islands of identical crystal structure are expected to couple, forming symmetric and anti-symmetric photonic envelope function states.

Numerical simulations demonstrate splitting of the out-of-phase lowest loss supermode of a single island into bonding and antibonding states with envelope functions confined in both islands [Fig. 3(a)]. The envelope function of the antibonding state exhibits a node at the center of the heterobarrier, whereas the bonding state does not vanish there. The difference in relative phase of the envelope functions of the bonding and antibonding states at the islands is

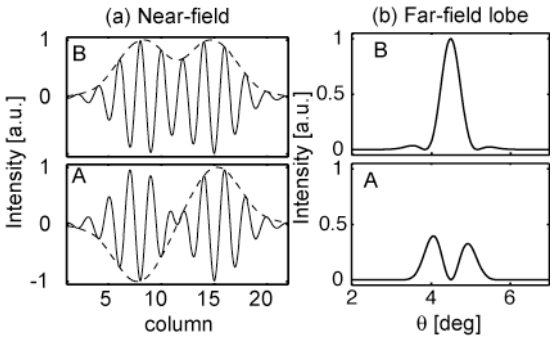

Fig. 3: (a) Calculated near and far-field (b) line scans of the bonding (B) and anti-bonding (A) modes of two 5×5 photonic island separated by 2 lattice periods. Other parameters are as for Fig. 2.

manifested by different characteristic far-field patterns [Fig. 3(b)]. It can be seen that the interference of the emission from the coupled islands produces additional features in the main far-field lobes obtained for an individual island [compare Fig 2(b,d)]. In the bonding state, the two envelope functions of the islands are in phase, producing a bright intensity fringe at the center of each lobe. Conversely, for the antibonding state the envelope function at the two islands is out-of-phase, resulting in a dark fringe at the center of the lobes.

The system of two closely placed photonic islands is an example of a lattice where an additional periodicity is superimposed on the heterostructure scale. In fact, a PhCH superlattice (SL) can be formed by constructing an array of coupled islands, for which the island supermodes would split in a PhCH SL miniband. Figure 4 illustrates this for three coupled photonic islands. As in the case of two photonic islands, the lowest loss mode maintains the out-of-phase relationship between adjacent lattice sites. This is because the higher order modes have envelope functions that exhibit nodes within the array. This either forces the amplitude of a column to vanish or renders two columns in phase, which in both cases increases the modal losses.

The difference in envelope functions of the three modes is manifested by different characteristic far-field patterns [Fig 4(b)]. The fine structure of the main far-field lobe now shows a splitting into additional fringes, as compared to the single and two-island far-field lobes. These characteristic signatures of the lowest loss modes make it possible to experimentally distinguish between the modes.

Tuning of two photonic islands

In the case of two-coupled islands, lasing on the bonding envelope-function mode was observed as the system was driven by a single electrical contact [9]. However, the fabrication of identical photonic islands is limited by the resolution of the lithography technique and by nonuniformities of the VCSEL wafer. There are thus inadvertent differences between

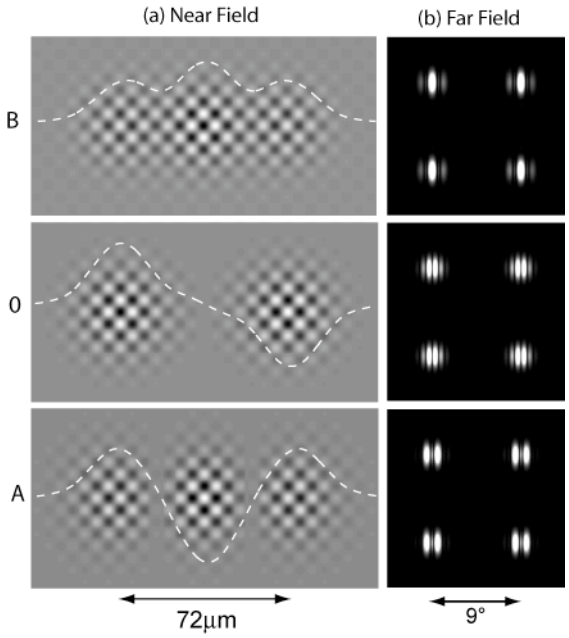

Fig. 4: (a) Calculated near and far-field (b) pattern of the "bonding" (B), "zeroth" (0) and "anti-bonding" (A) modes of three 5x5 photonic island, each separated by 2 lattice periods. The dashed curve is the slowly varying envelope function along the center of the array. All other parameters are as for Fig. 2.

the islands, resulting in weaker effective coupling between them and, in turn, to localization of the envelope function at either island. The dissimilarities between the islands can be compensated for by modifying the gain at each island, which may be achieved by injecting different currents into separated parts of the array. Separate contacting can thus be useful in bringing the two islands into resonance and inducing efficient coupling. Alternatively, current control of the coupling may be used to change the localization of the photonic mode, which can yield beam switching.

We have fabricated separate-contact coupled islands such that two different currents can be fed into each island while avoiding significant changes in the mirror reflectivity pattern across the PhCH. In order to keep the periodic reflectivity pattern, the two contact pads were aligned with the lattice defining the PhC. Removing the Cr grid between two pixel columns in the barrier between the islands separated the two contacts, Fig.1. The locally removed Cr grid slightly perturbs the periodic reflectivity pattern. In order to minimize this perturbation, the unpatterned top distributed Bragg reflector separating the two contacts was etched such as to imitate the reflectivity of the missing Cr patterned grid.

Figure 5 demonstrates the lasing characteristics of such VCSEL-based PhCH system incorporating two 4×5 photonic islands using two separated contact pads. The VCSEL-based PhCH was pulse-driven, with a repetition rate of 100kHz and 50 ns wide

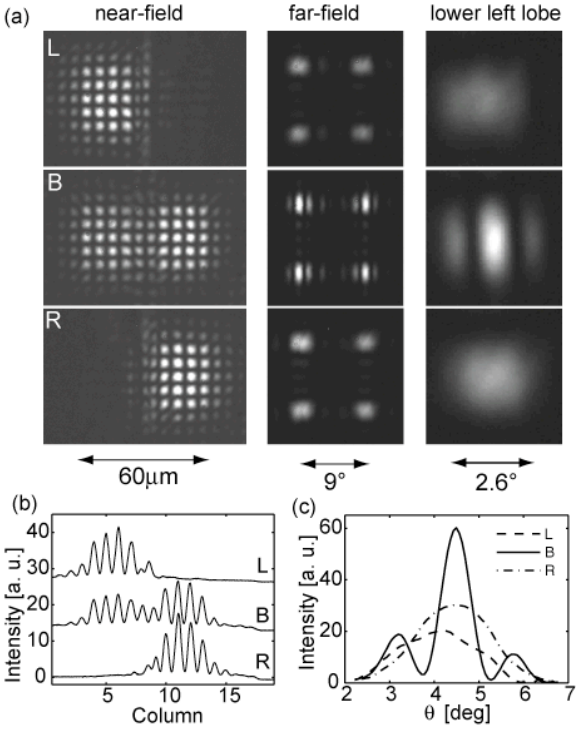

Fig. 5: Emission characteristics of separate-contact PhCHs incorporating two 4×5 coupled islands separated by 2 lattice periods. (a) Near-field patterns corresponding to current injection in the left (L), right (R) and both of the photonic islands (B) and corresponding far-field patterns (The light from the "sea" domain was blocked). (b) Average line scans across the near-field patterns of (a). (c) Average line scans of the lower left far-field lobes in (a).

pulses. Injection into the left side of the array (L) leads to photonic envelope function localization in the island situated there. Switching the current to the right contact yields switching of the envelope function to the right island. Coupling between the islands was achieved by synchronizing the electrical pulses in time and adjusting their relative magnitudes. In this way, we achieved lasing at both islands with preserved periodicity of the optical mode across the entire array, [Fig 5(a,b), B].

The switching between coupled and uncoupled coupling PhCH islands is corroborated by the measured far field patterns shown in Fig 5(a). For single island operation, the PhCH lases on the lowest loss out-of-phase supermode with a characteristic four-lobe far-field pattern, indicating a π phase shift between neighboring lattice sites. The mutual coherence between the coupled islands is manifested by the fine structure splitting of the main far-field lobes. In particular, the occurrence of a bright fringe at the center of each main lobe evidences lasing on the bonding state, as predicted by the calculations presented above. Of special interest is also the far-field position where the beam of the coupled structure exhibits a null, since bringing the islands in and out of coupling modulates the optical field there with high modulation contrast.

The coupling of the envelope functions of the two islands is also characterized by "wavelength alignment" among the array element, as shown by the measured, spectrally resolved near-field patterns in Fig. 6(a). These patterns were generated by focusing one row in the center of the PhCH onto the input slit of a spectrometer. For individual operation of the islands, each island lases generally at a different wavelength. The elements within each array side are however locked to the same wavelength. By proper adjustment of the two currents, the wavelength of the resulting coherent supermode could be locked into a single spectral line [see Fig.6(a,b)]. The wavelength of the coupled system is red-shifted with respect to the lasing wavelengths of the solitary islands. Thus, the emission wavelength of the coupled structure can be electrically tuned by changing the two injected currents.

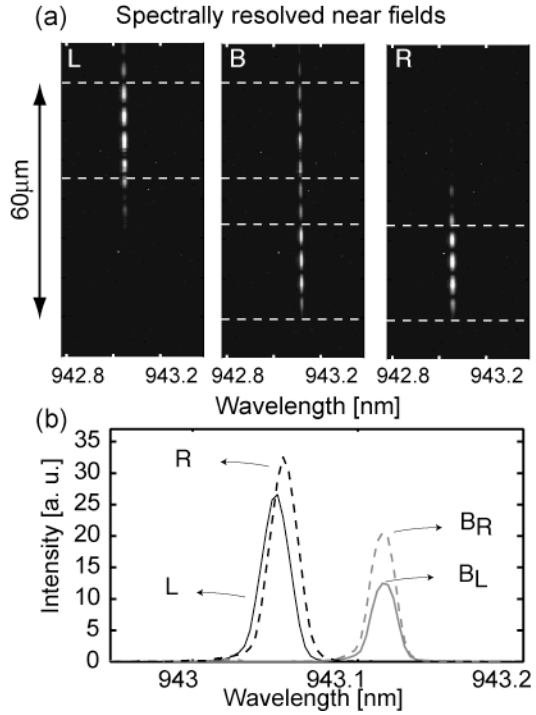

Fig. 6: (a) Spectrally resolved near-field of one row of the coupled PhCH islands of Fig. 5 corresponding to current injection in the left (L), right (R) and both (B) photonic island(s). (b) Line scans across the spectra (averaged between the white dashed lines) in (a). The index notation B_L and B_R relates to the spatial positions corresponding to the left and right islands, respectively.

Photonic Superlattices

In addition to the system of two photonic islands, we have fabricated arrays incorporating three, separately contacted photonic islands, [see Fig. 1]. As in the case of the double-contact structures, control of the gain distribution was achieved by adjusting the currents injected into each island. By proper adjustment of the currents, the PhCH SL can be brought to lase at mainly one SL mode where the separated islands are mutually coherent. Small

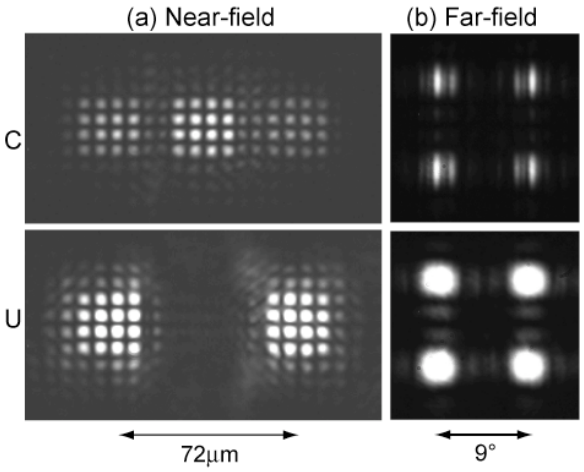

Fig. 7: Measured near (a) and far-field (b) patterns of coupled (C) and uncoupled (U) PhC SLs. I_L=690 mA, I_R=700 mA, I_M=0 mA (U) and I_M=380mA (C).

changes in the currents can break the coupling, with a subsequent significant change in the near and far-field pattern.

Figure 7 depicts the measured near and far-field patterns of the PhCH SL as it is brought in and out of coupling by adjusting the current I_C through the center island. For I_C=0 and I_L=690 mA, I_R=700 mA (pulsed conditions), the left and right islands lase independently, and the far-field pattern shows the expected four-lobe pattern due to diffraction at each island. (The light from the "sea" domain was blocked in order to increase the lobe width). For I_C= 380 mA, the center island lases as well, and each far-field lobe splits into several narrow peaks. Comparison of the measured and calculated far-field profiles, (Fig. 8), shows that lasing under these conditions is mainly on the bonding SL mode, with weaker contributions from the A and 0 SL modes.

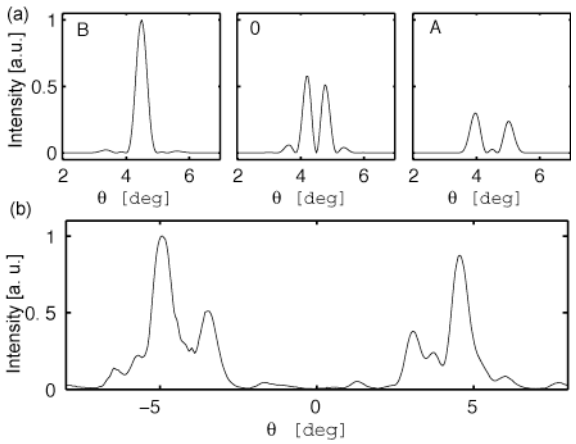

Fig. 8: (a) Calculated far-field line scans across the major lobes of the 3 lowest loss modes (B, 0, A) of Fig 4. (b) Measured line scan across the lower far-field lobes of Fig 7 in the coupled case.

Conclusion

Combining photonic envelope function confinement effects with active control of the gain distribution in VCSEL-based photonic crystal heterostructures brings about beam switching due to envelope function coupling and localization. We demonstrate coherent coupling of multiple heterostructure domains, resulting in significant modifications of the near-and far-field patterns. Controlling the envelope function modes in photonic crystal heterostructures and superlattices might be useful for applications such as optical beam steering and routing.

References

1 M. Orenstein, E. Kapon, N. G. Stoffel, J. P. Harbison, L. T. Fiorez, and J. Wullert, Appl. Phys. Lett, **58**, 804 (1991).
2 H. Pier, E. Kapon, and M. Moser, Nature **407**, 880 (2000).
3 L.J. Mawst, IEEE Circuits Devices Mag. **19**, 34 (2003)
4 M. Dabbicco, T. Maggipinto, and M. Brambilla, Appl. Phys. **86**, 021116 (2005).
5 A. Golshani, H. Pier, E. Kapon, and M. Moser, J. Appl. Phys. **85**, 2454 (1999).
6 D. L. Boiko, G. Guerrero, and E. Kapon, Optics Express, **12**, 2597 (2004).
7 C.-A. Berseth, G. Guerrero, E. Kapon, M. Moser, and R. Hövel, Conference on Lasers and Electro-Optics (CLEO), San Francisco, 7-12 May 2000, (Optical Society of America, Washington, D.C., 2000), pp 171-172.
8 G. Guerrero, D. L. Boiko, and E. Kapon, Optics Express, **12**, 4922, (2004).
9 L.D.A. Lundeberg, D.L. Boiko, and E. Kapon, Appl. Phys. Lett. **87**, 241120 (2005)